An Adaptive Nonlinear Controller for DFIM-Based Wind Energy Conversion Systems

Juan Manuel Mauricio, *Student Member, IEEE*, Andrés E. León, *Student Member, IEEE*, Antonio Gómez-Expósito, *Fellow, IEEE*, and Jorge A. Solsona, *Senior Member, IEEE*

***Abstract*—An adaptive nonlinear controller for wind energy doubly fed induction machines is introduced in this paper. The proposed controller is based on the feedback linearization technique and includes a disturbance observer for estimation of parameter uncertainties. Estimated uncertainties values are injected in order to construct the control law, improving in this way the system's performance. The controller behavior, when tracking power references, is tested with realistic Electromagnetic Transients for dc /Power Systems Computer-Aided Design simulations. In addition, the controller performance is checked in the presence of parameter uncertainties and nearby faults.**

***Index Terms*—Doubly fed induction machine (DFIM), feedback linearization (FL), nonlinear observer, voltage source converter (VSC), wind energy conversion (WEC).**

I. Introduction

THE INCREASINGLY widespread use of wind generation in power networks imposes the requirement that wind farms should be able to contribute to network support and operation, much in the same way as conventional generating stations based on synchronous generators do [1]. Actual grid codes for wind farm connection demand high performance of connected plants with respect to voltage and power control ability, as well as fault ride through capability [2].

The doubly fed induction machine (DFIM) is able to control its active and reactive power outputs as required by system operators. Although the active power depends on the energy transferred from the wind, it can be controlled in a transient manner by resorting to the mechanical system kinetic energy. In addition, these machines can work at asynchronous speeds, increasing in this way the wind energy transfer efficiency for a given wind speed while the mechanical stress is relieved to a certain extent. In this paper, the transient behavior of the DFIM is considered in order to improve its own transient response and bring possible network support [3], [4].

The model of the DFIM belongs to the nonlinear multiple-input multiple-output class. Throughout its life a wind farm can operate in a wide range of active and reactive generated powers. Therefore, linear control strategies [5], [6], assuming small power excursions around an equilibrium point, face difficulties when designing appropriate gains to assure nonlinear system stability, particularly considering the need of using high gain values to maintain a good performance control under important perturbations. In industrial applications, vector control is often used [7]. This strategy allows active and reactive powers to be independently controlled via an asymptotic decoupling. The increasingly competitive nature of the wind farms market and the severe regulations imposed on them are leading industry to find new high-performance control strategies. For this reason, several nonlinear complex strategies have been proposed by researchers. For instance, a nonstructured control model applied to the DFIM, based on a fuzzy logic approach, can be found in [8]. Interconnection and damping assignment and back-stepping control are used in [9] and [10], respectively, while a direct power control strategy is proposed in [11] .

Feedback linearization (FL) controllers have shown an excellent performance in controlling nonlinear systems. Under this strategy, which transforms the original nonlinear system into decoupled linear systems, the controller tuning is performed via linear control laws [12], [13]. This method allows nonlinear controllers to be easily designed so that good performance is guaranteed for a wide range of operating points. This technique was applied to the DFIM wind farms in [14] and [15], by assuming an exact knowledge of model parameters. However, besides the nonlinearities related to measurement noise and harmonic pollution originating in the supply converters, electrical machine parameters are strongly affected by temperature, saturation, and skin effects, which can deteriorate the controller performance when designed with nominal parameter values. In order to compensate for these uncertainties, adaptive controllers are implemented to improve the system performance. For instance, a drive including a DFIM is controlled in [16] by using a sliding-mode controller adapted to changes in machine resistances.

In this paper, an adaptive nonlinear control strategy for DFIM-based wind energy conversion (WEC) system is developed in order to attenuate the effect of parameter uncertainties arising in the model. This is performed by including a disturbance observer in the control law that estimates the model uncertainties (changes in resistances, inductances, and other parameters of the DFIM and their converters), and then injects them into the controller under a feedforward scheme, canceling their effect in a faster manner. Furthermore, in our proposal, the equation system characterizing the rotor currents dynamics is exactly

Manuscript received January 16, 2008. Current version published November 21, 2008. This work was supported in part by the Spanish Ministry of Education and Science (MEC) and Junta de Andalucía under Grants DPI2001-2612 and Grant ACC-1021-TIC-2002, respectively and in part by the Universidad Nacional del Sur, Consejo Nacional de Investigaciones Científicas y Técnicas (CONICET) and Agencia Nacional de Promoción Científica y Tecnológica (ANPCyT), Argentina. Paper no. TEC-00323-2007.

J. M. Mauricio and A. G. Expósito are with the University of Seville, Seville 41004, Spain (e-mail: j.m.mauricio@ieee.org; age@us.es).

A. E. León and J. A. Solsona are with the Instituto de Investigaciones en Ingeniería Eléctrica (IIIE), Universidad Nacional del Sur (UNS)-Consejo Nacional de Investigaciones Científicas y Técnicas (CONICET), Departamento de Ingeniería Eléctrica y de Computadoras, Universidad Nacional del Sur, Bahía Blanca 8000, Argentina (e-mail: andreseleon@gmail.com; jsolsona@uns.edu.ar).

Digital Object Identifier 10.1109/TEC.2008.2001441

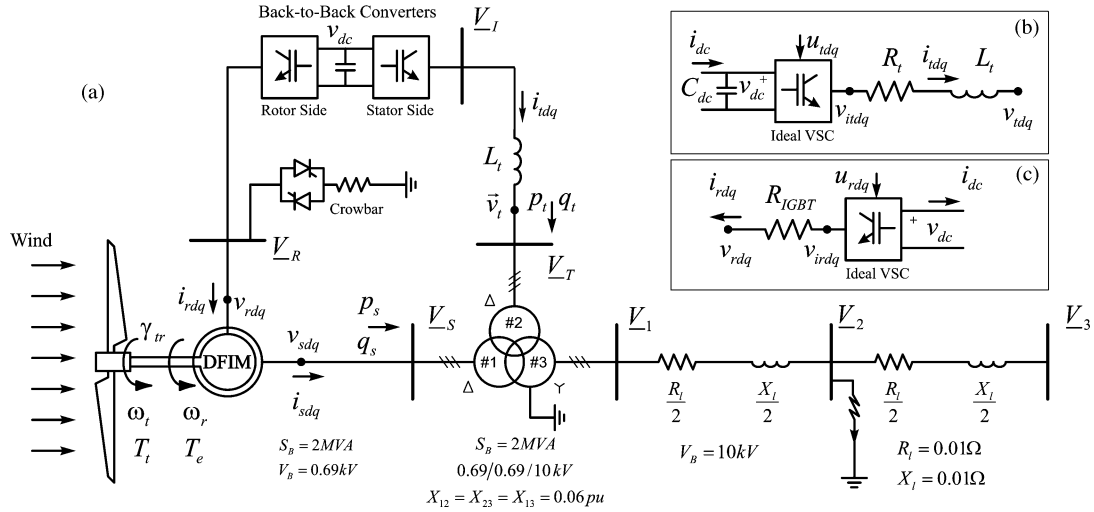

Fig. 1. DFIM-based WEC system.

linearized and decoupled. Then, through a cascaded approach, DFIM's stator currents are controlled. These currents have a direct relationship with stator active and reactive powers. When the system is tested in tracking power references and mitigating fault conditions, this strategy performs better than classical vector control.

The control strategy is tested through simulations performed on realistic models by using Electromagnetic Transients for dc (EMTDC)/Power Systems Computer-Aided Design (PSCAD). The test system consists of a 2-MW generator, equipped with pulse width modulation (PWM) voltage source converters (VSCs). The system behavior when tracking active and reactive power references is shown. As described in the literature, controllers must present not only a good reference tracking capability but also a good disturbance rejection under grid faults or other common perturbations [17]. For this reason, the behavior of our controller is tested in the presence of this kind of disturbances. In addition, a comparison between the proposed strategy and vector control is performed.

The rest of the paper is organized as follows. In Section II, the DFIM and VSC models are presented. The control strategy design is described in Section III, while performance tests, discussion, and results are shown in Section IV. Finally, conclusions are given in Section V.

II. Model

The system considered, shown in Fig. 1(a), is a WEC system based on a DFIM [18]. It consists of a wind turbine connected through a nonrigid shaft to the DFIM's rotor. Other major blocks are the back-to-back VSCs and the thyristor-based crowbar protection system. The stator is connected through a step-up three-winding transformer to the distribution grid. One of the transformer windings feeds the stator-side VSC. It is considered that the active and reactive powers are measured at bus 1, i.e., at the 10 kV side of the transformer. Each device composing this WEC system is going to be modeled separately in the next sections.

A. Electrical DFIM Model

In a synchronously rotating reference frame, the equations in per unit (p.u.) describing a DFIM are [19]

$$\Gamma \dot{i}_{sd} = -L_r\left(R_s i_{sd} + v_{sd}\right) - \Gamma\Omega_B\omega_s i_{sq} + L_m\left(R_r i_{rd} + v_{rd} - \omega_r\left(L_m i_{sq} + L_r i_{rq}\right)\right) \quad (1)$$

$$\Gamma \dot{i}_{sq} = -L_r\left(R_s i_{sq} + v_{sq}\right) + \Gamma\Omega_B\omega_s i_{sd} + L_m\left(R_r i_{rq} + v_{rq} + \omega_r\left(L_m i_{sd} + L_r i_{rd}\right)\right) \quad (2)$$

$$\Gamma \dot{i}_{rd} = L_m\left(R_s i_{sd} + v_{sd}\right) - \Gamma\Omega_B\omega_s i_{rq} - L_s\left(R_r i_{rd} + v_{rd} - \omega_r\left(L_m i_{sq} + L_r i_{rq}\right)\right) \quad (3)$$

$$\Gamma \dot{i}_{rq} = L_m\left(R_s i_{sq} + v_{sq}\right) + \Gamma\Omega_B\omega_s i_{rd} - L_s\left(R_r i_{rq} + v_{rq} + \omega_r\left(L_m i_{sd} + L_r i_{rd}\right)\right) \quad (4)$$

with

$$\Gamma \triangleq \Omega_B^{-1}\left(L_s L_r - L_m^2\right) \quad (5)$$

$$L_s \triangleq L_m + L_{ls} \quad (6)$$

$$L_r \triangleq L_m + L_{lr} \quad (7)$$

where

Ω_B	base angular frequency [rad/s];
ω_s	synchronous frequency [p.u.];
ω_t, ω_r	turbine and DFIM rotor speeds [p.u.];
v_{sd}, v_{sq}	dq stator voltages [p.u.];
v_{rd}, v_{rq}	dq rotor voltages [p.u.];
i_{sd}, i_{sq}	dq stator currents [p.u.];
i_{rd}, i_{rq}	dq rotor currents [p.u.];
L_s, L_r	stator and rotor self inductances [p.u.];
L_m	stator–rotor mutual inductance [p.u.];
L_{ls}, L_{lr}	stator and rotor leakage inductance [p.u.];
R_s, R_r	stator and rotor resistances [p.u.];
Γ	constant parameter [s/rad].

B. Mechanical System

The aim of this paper is to control the active and reactive powers provided by the WEC system from a transient point of view. In steady state, the active power injected to the grid depends on the power supplied by the wind. However, active power injections can be introduced transiently. This power is supplied by the kinetic energy of the turbine, gear box, and rotor masses. For this reason, it is crucial to model the mechanical system of the WEC system. A two-mass lumped model is used to represent the mechanical dynamics, as proposed in [20]

$$\dot{\gamma}_{tr} = \Omega_B \left(\omega_r - \omega_t\right) \tag{8}$$

$$2H_t\dot{\omega}_t = T_t - K_{tr}\gamma_{tr} - D_{tr}\left(\omega_t - \omega_r\right) \tag{9}$$

$$2H_r\dot{\omega}_r = K_{tr}\gamma_{tr} - T_e - D_{tr}\left(\omega_r - \omega_t\right) \tag{10}$$

with

$$T_e = \frac{3}{2}L_m\left(i_{sq}i_{rd} - i_{sd}i_{rq}\right) \tag{11}$$

where

γ_{tr}	angle between turbine and DFIM rotor [rad];
H_t, H_r	turbine and DFIM rotor inertias [s];
K_{tr}	shaft stiffness [p.u.];
D_{tr}	shaft mutual damping [p.u.];
T_t	mechanical torque [p.u.];
T_e	electrical torque [p.u.].

In these equations, the mechanical torque T_t, generated by the wind, is considered constant because this paper focuses on a short period of time.

C. Voltage Source Converters

It is common not to include the converter models when simulating DFIM behavior, under the assumption that the converter response is fast enough and its energy consumption is relatively low compared with the power that flows from the stator. However, the stator response speed arising from the high-performance controller developed in this paper is close to the converter speed. In addition, the operation of the controller during fault is taken into account. For this reason, the interaction between DFIM, grid, and converters is included in the model.

1) Stator-Side Converter: The stator-side converter has two tasks, the most important being to maintain the dc voltage constant under different network and WEC system conditions. Another task to be performed by this converter is the injection of reactive power on the stator-side bus. This injection could help in the presence of faults. Although, for simplicity, the reactive power is held null in this paper, its use to track a given reference is straightforward.

The model considered, shown in Fig. 1(b), consists of an insulated gate bipolar transistor (IGBT) bridge connected on the left side to the dc capacitor and on the right side to the network, through an equivalent resistance and coupling inductance. The converter is based on IGBTs whose relatively high resistance cannot be neglected. It is included in the equivalent resistance R_t.

The model for this VSC takes into account the dc voltage and dq currents dynamics as follows:

$$\frac{1}{\Omega_B}L_t\dot{i}_{td} = -R_t i_{td} - L_t\omega_t i_{tq} + \eta_{td}v_{dc} - v_{td} \tag{12}$$

$$\frac{1}{\Omega_B}L_t\dot{i}_{tq} = -R_t i_{tq} + L_t\omega_t i_{td} + \eta_{tq}v_{dc} - v_{tq} \tag{13}$$

$$\frac{1}{\Omega_B}C_{dc}\dot{v}_{dc} = -\frac{3}{2}\left(\eta_{td}i_{td} + \eta_{tq}i_{tq}\right) + i_{dc} \tag{14}$$

where

L_t, R_t	equivalent VSC inductance and resistance [p.u.];
$C_{\rm dc}$	dc-link capacitance [p.u.];
$v_{\rm dc}$	dc-link voltage [p.u.];
i_{td}, i_{tq}	stator-side VSC dq currents [p.u.];
v_{td}, v_{tq}	stator-side VSC dq voltages [p.u.];
η_{td}, η_{tq}	stator-side VSC dq switching state functions.

2) Rotor-Side Converter: The rotor-side converter, whose equivalent model is shown in Fig. 1(c), yields the voltages required by the DFIM controller. As in the case of the stator-side VSC, IGBT resistances are not neglected but added to the DFIM rotor resistance in order to be taken into account by the proposed controller. The resulting equivalent resistance not only depends on the temperature but also on the commutation frequency and duty cycle. This uncertainty should be considered by the controller, as proposed in the following sections.

III. Disturbance Compensation Control Strategy

A. Modeling of Parameter Uncertainties

There is always a degree of uncertainty in the parameters of the system components as well as nonmodeled dynamics that can affect the controller performance. In this paper, a controller for improved performance in the presence of uncertainties is to be designed. In order to proceed with the design (see next sections), parameter uncertainties are modeled as follows. Let P denote a generic parameter so that $P \in \{R_r, R_s, L_m, L_s, L_r, \Gamma\}$ represents the set of all possible parameters. The actual parameter value can be written as a perturbation from its nominal or assumed value, $P = P_0 + \Delta P$. In this way, the rotor current dynamics (3) and (4) can be rewritten as a function of their known parameter values, denoted by subindex 0, plus a term Δ_i that groups all of the uncertainties

$$\dot{i}_{rd} = \frac{L_{m0}}{\Gamma_0}\left(R_{s0}i_{sd} + v_{sd}\right) - \Omega_B\omega_s i_{rq} + \Delta_1 - \frac{L_{s0}}{\Gamma_0}\left(R_{r0}i_{rd} + v_{rd} - \omega_r\left(L_{m0}i_{sq} + L_{r0}i_{rq}\right)\right) \tag{15}$$

$$\dot{i}_{rq} = \frac{L_{m0}}{\Gamma_0}\left(R_{s0}i_{sq} + v_{sq}\right) + \Omega_B\omega_s i_{rd} + \Delta_2 - \frac{L_{s0}}{\Gamma_0}\left(R_{r0}i_{rq} + v_{rq} + \omega_r\left(L_{m0}i_{sd} + L_{r0}i_{rd}\right)\right). \tag{16}$$

Note that $\Delta_i = \Delta_i(\Delta P, i_r, i_s, v_r, v_s)$.

B. Proposed Nonlinear Controller

In order to apply the feedback linearization theory [21], an input transformation is performed by defining the following auxiliary control inputs:

$$u_{rd} = \frac{L_{m0}}{\Gamma_0}\left(R_{s0}i_{sd} + v_{sd}\right) - \Omega_B\omega_s i_{rq} + \Delta_1 - \frac{L_{s0}}{\Gamma_0}\left(R_{r0}i_{rd} + v_{rd} - \omega_r\left(L_{m0}i_{sq} + L_{r0}i_{rq}\right)\right) \quad (17)$$

$$u_{rq} = \frac{L_{m0}}{\Gamma_0}\left(R_{s0}i_{sq} + v_{sq}\right) + \Omega_B\omega_s i_{rd} + \Delta_2 - \frac{L_{s0}}{\Gamma_0}\left(R_{r0}i_{rq} + v_{rq} + \omega_r\left(L_{m0}i_{sd} + L_{r0}i_{rd}\right)\right) \quad (18)$$

where the subindex 0 indicates nominal parameter values, and Δ_1 and Δ_2 are the uncertainty terms appearing in (15) and (16). Δ_1 and Δ_2 were included in the control law to improve the system performance. In this case, from (17) and (18), rotor current dynamics [(15) and (16)] becomes linear and decoupled

$$\dot{i}_{rd} = u_{rd} \quad (19)$$

$$\dot{i}_{rq} = u_{rq}. \quad (20)$$

Then, (19) and (20) are linear systems of the form $\dot{x} = u$ for which linear control techniques can be designed. By defining the tracking error as $e = x - x^\star$, the error dynamics turns out to be $\dot{e} + ke = 0$. Finally, the control law defining the new inputs u_{rd} and u_{rq} becomes

$$u_{rd} = \dot{i}^\star_{rd} - k_{rd}\left(i_{rd} - i^\star_{rd}\right) \quad (21)$$

$$u_{rq} = \dot{i}^\star_{rq} - k_{rq}\left(i_{rq} - i^\star_{rq}\right). \quad (22)$$

The control inputs to be applied in the rotor (v_{rd} and v_{rq}) obtained from (17) and (18) result in

$$v_{rd} = \frac{\Gamma_0}{L_{s0}}\left(\Omega_B\omega_s i_{rq} - \hat{\Delta}_1 + u_{rd}\right) + R_{r0}i_{rd} - \omega_r\left(L_{m0}i_{sq} + L_{r0}i_{rq}\right) - \frac{L_{m0}}{L_{s0}}\left(R_{s0}i_{sd} + v_{sd}\right) \quad (23)$$

$$v_{rq} = \frac{\Gamma_0}{L_{s0}}\left(-\Omega_B\omega_s i_{rd} - \hat{\Delta}_2 + u_{rq}\right) + R_{r0}i_{rq} + \omega_r\left(L_{m0}i_{sd} + L_{r0}i_{rd}\right) - \frac{L_{m0}}{L_{s0}}\left(R_{s0}i_{sq} + v_{sq}\right) \quad (24)$$

where $\hat{\Delta}_1$ and $\hat{\Delta}_2$ denote estimated values. Note that Δ_1 and Δ_2 are unknown, then in the proposed controller, these values are replaced by estimated values [see (23) and (24)] obtained from measured variables. These estimates will be calculated in the next section.

From the earlier controller, it is possible to control rotor currents independently. Although these currents have no practical importance, they can be used to control stator currents in a cascaded approach. The stator currents are relevant because they define the active and reactive power injected by the DFIM to the grid. From (25) and (26), the rotor current references can be obtained from the desired stator currents

$$i^\star_{rd} = k_d\left(i_{sd} - i^\star_{sd}\right) + \frac{k_d}{\tau_{id}}\int_0^t \left(i_{sd} - i^\star_{sd}\right)dt \quad (25)$$

$$i^\star_{rq} = k_q\left(i_{sq} - i^\star_{sq}\right) + \frac{k_q}{\tau_{iq}}\int_0^t \left(i_{sq} - i^\star_{sq}\right)dt. \quad (26)$$

Applying pq theory [22], the stator current references can be calculated from the active and reactive desired powers to be injected by the DFIM

$$i^\star_{sd} = \frac{v_{sd}p^\star_s - v_{sq}q^\star_s}{v^2_{sd} + v^2_{sq}} \quad (27)$$

$$i^\star_{sq} = \frac{v_{sd}q^\star_s + v_{sq}p^\star_s}{v^2_{sd} + v^2_{sq}}. \quad (28)$$

It is important to remark that the active power is imposed by the power transferred from the wind to the WEC system. However, taking advantage of the kinetic energy stored in the mechanical components, the power injected to the grid can be transiently controlled in a flexible manner. In the case of the WEC system, the inertia of its rotating masses is relatively high; therefore, important amounts of power can be obtained from them. In steady state, the controller objective should be to obtain the highest transfer efficiency from the wind, which is achieved through the speed, rather than the active power control. For this objective, the global control strategy can be designed through an inner loop controlling active power and an outer and slower loop controlling speed. As only the transient behavior is analyzed in this paper, the emphasis is put on the fast inner loop.

C. Nonlinear Disturbance Observer Design

In order to design the compensation terms $\hat{\Delta}_1$ and $\hat{\Delta}_2$, a reduced-order disturbance observer is built. To this end, the following procedure is used. An extended model, assuming slow-varying machine parameters, is first obtained. Then, linear and nonlinear parts of (15) and (16) are split as follows:

$$\begin{bmatrix}\dot{\mathbf{x}}_a \\ \hline \dot{\mathbf{x}}_b\end{bmatrix} = \left[\begin{array}{c|c}\mathbf{A}_{aa} & \mathbf{I} \\ \hline 0 & 0\end{array}\right]\begin{bmatrix}\mathbf{x}_a \\ \hline \mathbf{x}_b\end{bmatrix} + \begin{bmatrix}\mathbf{B}_{au} \\ \hline \mathbf{0}\end{bmatrix} \quad (29)$$

where (*), as shown at the bottom of the next page, and $\mathbf{I} \in \mathbb{R}^{2\times 2}$ is the identity matrix. Finally, based on the earlier model, a reduced-order nonlinear observer is proposed. It has the following structure:

$$\dot{\boldsymbol{\xi}} = -\mathbf{G}_p\left(\boldsymbol{\xi} + \left(\mathbf{G}_p + \mathbf{A}_{aa}\right)\mathbf{x}_a + \mathbf{B}_{au}\right) \quad (30)$$

$$\hat{\mathbf{x}}_b = \boldsymbol{\xi} + \mathbf{G}_p\mathbf{x}_a \quad (31)$$

where $\boldsymbol{\xi} \in \mathbb{R}^{2\times 1}$ is the observer state vector and $\mathbf{G}_p \in \mathbb{R}^{2\times 2}$ is the observer gain matrix, designed as a trade-off between measurement noise and estimation error convergence rate.

Defining the error as $\mathbf{e} = \mathbf{x}_b - \hat{\mathbf{x}}_b$, it is not difficult to prove that its dynamics are governed by the following linear expression,

$$\dot{\mathbf{e}} = -\mathbf{G}_p\mathbf{e}. \quad (32)$$

Therefore, the gain $\mathbf{G}_p$ can be calculated by linear techniques, like pole placement, quadratic optimization techniques, etc.

Note that $\hat{\mathbf{x}}_b = [\hat{\Delta}_1 \quad \hat{\Delta}_2]^T$ [see $\mathbf{x}_b$ definition in (29)]. These estimates are used in the control process [see (23) and (24)].

D. VSC Controller

The control strategy applied to the VSC is based on the input–output exact linearization, choosing the currents as outputs. With this choice, currents remain decoupled through the crossed feedforward loops, while the capacitor voltage remains within the stable internal dynamics. This voltage is controlled by an additional control loop in cascade with the current i_{tq}. The design methodology is as follows. First of all, the following auxiliary inputs are defined:

$$u_{td} = \frac{\Omega_B}{L_t}\left(-R_t i_{td} - L_t \omega_t i_{tq} + \eta_{td} v_{dc} - v_{td}\right) \quad (33)$$

$$u_{tq} = \frac{\Omega_B}{L_t}\left(-R_t i_{tq} + L_t \omega_t i_{td} + \eta_{tq} v_{dc} - v_{tq}\right) \quad (34)$$

$$u_{dc} = \frac{\Omega_B}{C_{dc}}\left(-\frac{3}{2}\left(\eta_{td} i_{td} + \eta_{tq} i_{tq}\right) + i_{dc}\right). \quad (35)$$

Replacing (33)–(35) in (12)–(14), the dynamics are transformed into decoupled linear equations

$$\dot{i}_{td} = u_{td} \quad (36)$$

$$\dot{i}_{tq} = u_{tq} \quad (37)$$

$$\dot{v}_{\rm dc} = u_{\rm dc}. \quad (38)$$

Thus, closed-loop control laws can be designed to track references much like in the rotor currents dynamics case [(19) and (20)]. Consequently,

$$u_{td} = \dot{i}^{\star}_{td} - k_{td}\left(i_{td} - i^{\star}_{td}\right) \quad (39)$$

$$u_{tq} = \dot{i}^{\star}_{tq} - k_{tq}\left(i_{tq} - i^{\star}_{tq}\right) \quad (40)$$

$$u_{\rm dc} = \dot{v}^{\star}_{\rm dc} - k_{\rm dc}\left(v_{\rm dc} - v^{\star}_{\rm dc}\right) - \frac{k_{\rm dc}}{\tau_{i\rm dc}}\int\left(v_{\rm dc} - v^{\star}_{\rm dc}\right)dt \quad (41)$$

the references being the desired value for each state variable.

The control inputs η_{td} and η_{tq} are recovered from (33) and (34) resulting in,

$$\eta_{td} = \frac{1}{v_{dc}}\left(R_t i_{td} + L_t \omega_t i_{tq} + v_{td} + \frac{L_t}{\Omega_B} u_{td}\right) \quad (42)$$

$$\eta_{tq} = \frac{1}{v_{dc}}\left(R_t i_{tq} - L_t \omega_t i_{td} + v_{tq} + \frac{L_t}{\Omega_B} u_{tq}\right) \quad (43)$$

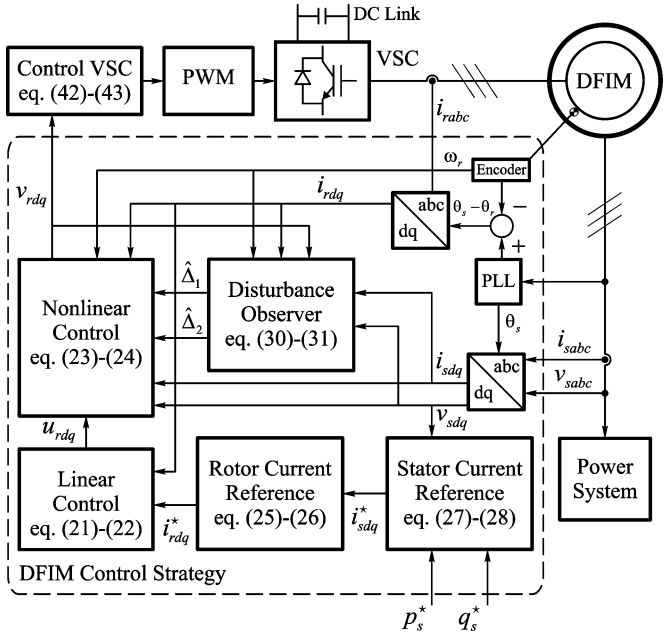

Fig. 2. Proposed control strategy (block diagram).

Since the q-axis at the point of connection with the grid was chosen as the reference in the Park transformation, then $v_{td} = 0$ and $v_{tq} = V_t/\sqrt{3/2}$. Therefore, the active power demanded by the converter, in order to maintain the desired dc voltage level, will be given by the action of i_{tq}, while i_{td} is proportional to the desired injected reactive power. Next, a procedure that gives the expression for the reference current $i^{\star}_{tq}$ required to maintain a desired dc voltage [23] is provided. As the current dynamics are faster than the capacitor voltage dynamics, it can be assumed that currents will stabilize faster; therefore, from (12) and (13)

$$\eta_{td} v_{\rm dc} \cong L_t \omega_t i_{tq} + v_{td} \quad (44)$$

$$\eta_{tq} v_{\rm dc} \cong -L_t \omega_t i_{td} + v_{tq}. \quad (45)$$

Then, multiplying both sides of (35) by the capacitor voltage $v_{\rm dc}$, and using (44) and (45), the required expression is obtained

$$i^{\star}_{tq} = \frac{1}{v_{tq}}\left(\frac{2v_{\rm dc}}{3}\left(i_{\rm dc} - \frac{C_{\rm dc}}{\Omega_B} u_{\rm dc}\right) - v_{td} i_{td}\right). \quad (46)$$

Furthermore, by designing the current loop to respond much faster than the voltage loop, any major interaction between both control loops is prevented.

A block diagram representing the proposed nonlinear controller is shown in Fig. 2.

$$\mathbf{A}_{aa} = \begin{bmatrix} -\dfrac{L_{s0}R_{r0}}{\Gamma_0} & -\Omega_B\omega_s \\ \Omega_B\omega_s & \dfrac{-L_{s0}R_{r0}}{\Gamma_0} \end{bmatrix}, \qquad \mathbf{x}_a = \begin{bmatrix} i_{rd} \\ i_{rq} \end{bmatrix}, \qquad \mathbf{x}_b = \begin{bmatrix} \Delta_1 \\ \Delta_2 \end{bmatrix}$$

$$\mathbf{B}_{au} = \begin{bmatrix} \dfrac{L_{m0}}{\Gamma_0}\left(R_{s0} i_{sd} + v_{sd}\right) - \dfrac{L_{s0}}{\Gamma_0}\left(v_{rd} - \omega_r\left(L_{m0} i_{sq} + L_{r0} i_{rq}\right)\right) \\ \dfrac{L_{m0}}{\Gamma_0}\left(R_{s0} i_{sq} + v_{sq}\right) - \dfrac{L_{s0}}{\Gamma_0}\left(v_{rq} + \omega_r\left(L_{m0} i_{sd} + L_{r0} i_{rd}\right)\right) \end{bmatrix} \quad (*)$$

The vector control is the most commonly used in current DFIM-based WEC systems. It consists of transforming the stationary machine model to a rotating reference frame dq, and then, controlling active and reactive powers by the use of appropriate PI loops, through the rotor voltages. Although the vector control strategy is simpler, it shares with the proposed scheme the Park transformation and the pq theory computation. This means that at least a phase-lock loop (PLL) and rotor position sensor are needed. Hence, the proposed strategy can be implemented with the same hardware required by the vector control approach.

IV. Simulation Results

In order to show the proposed controller performance, several simulations were run with EMTDC/PSCAD. These simulations consider the most detailed DFIM model, including stator and rotor dynamics. Besides, PWM-controlled full IGBT models are adopted for the converters, instead of considering the average model simplification.

A. Active and Reactive Power Tracking

As mentioned before, the control objective is to track active and reactive power references. Although the steady-state active power is determined by the wind, the rotating masses of the mechanical system store kinetic energy that can be used to transiently inject a certain amount of active power. The use of this energy produces variations in the rotational speed that can be unacceptable. However, the high inertia of this kind of WEC systems (e.g., $H = 3\,\mathrm{s}$) allows noticeable active power variations to be achieved with relatively small changes in the machine speed. It is important to remark that these arbitrary injections are transient and must consider limitations such as axis mechanical stress, maximum allowed currents, voltages, etc. The adopted references have the following characteristics.

1) Step changes, to show the step response.
2) Relatively long time interval between step changes to show how the controllers can maintain a null tracking error, in spite of the state transients.
3) A potential future application of the power tracking capability could be in the power system oscillations damping [24]. These oscillations are a combination of sinusoids with frequencies ranging from 0.1 to 2.0 Hz. In order to properly damp such oscillations power injections with a greater bandwidth would be required. Therefore, sinusoids of 10 and 20 Hz are chosen as power references in order to test the controllers tracking capability.
4) Reactive power is tested in the two quadrants, i.e., generating and consuming, in order to show the controller flexibility for achieving power system operator requirements.
5) Important active power changes are imposed in order to show the high energy storing capacity of this WEC system.

The proposed power references are analytically provided in Table I and plotted in Fig. 3. In order to test the controllers against parameter uncertainty, the rotor-side equivalent resistance R_r is modified during the simulations. As explained before, this equivalent resistance includes, among others, the IGBT's resistance. Hence, the total resistance changes, for instance, when the rotor windings modify their temperature in accordance with the operating point or when the IGBT's duty cycle and commutation frequency are readjusted. The variation is a ramp that starts at 1.5 s and reach 50% at 2.5 s as in the fourth column of Table I. This test was also performed with other kind of resistance variations, such as exponential, sinusoids, temperature, commutation dependent, etc., but the ramp proved to be the most unfavorable.

TABLE I
Power References for Bus 1 and R_r Variation

Time (s)	$p_1^\star\ (MW)$	$q_1^\star\ (Mvar)$	$\Delta R_r\ (\%)$
0.0	2	0	0
0.5	1	0	0
1.0	1	-1	0
1.5	$3 + 0.5\sin(2\pi 10t)$	0	$50(t - 1.5)$
2.5	2	$-1 + 0.4\sin(2\pi 20t)$	50
3.0	3	$-1 + 0.4\sin(2\pi 20t)$	50
3.5	$2 + 0.4\sin(2\pi 10t)$	$0.5\sin(2\pi 20t)$	50

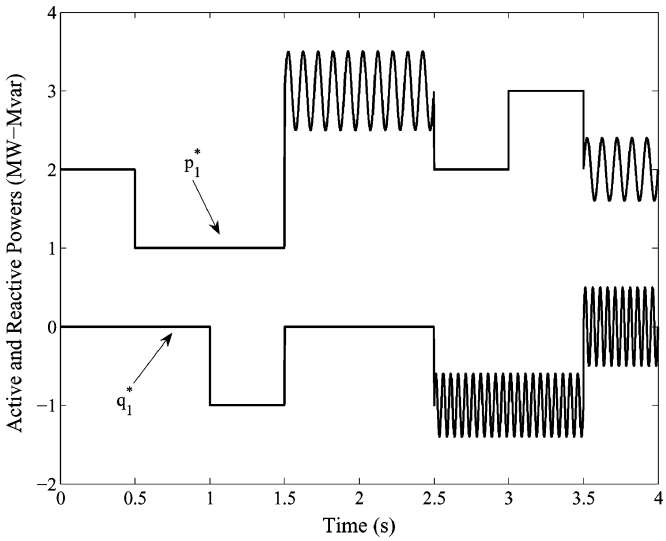

Fig. 3. Active and reactive power references.

In Fig. 4, the active power tracking errors of both the vector control approach and the proposed FL with Observer controller (FLO) are shown. There is a good tracking performance in most of the simulated responses with small errors. However, an increasing tracking error in active power can be observed for the vector control. This error arises when important speed changes are transiently imposed, like in this case, because the vector control cannot compensate for the speed voltage terms giving rise to the mentioned errors. It is important to remark that after a few seconds, the vector control is generally able to track these references without any error since it includes an integral term. On the other hand, the proposed controller shows in all situations a relatively small tracking error, which is not directly affected by the speed change.

In Fig. 5, the reactive power tracking errors of both approaches are shown. Although the vector control scheme

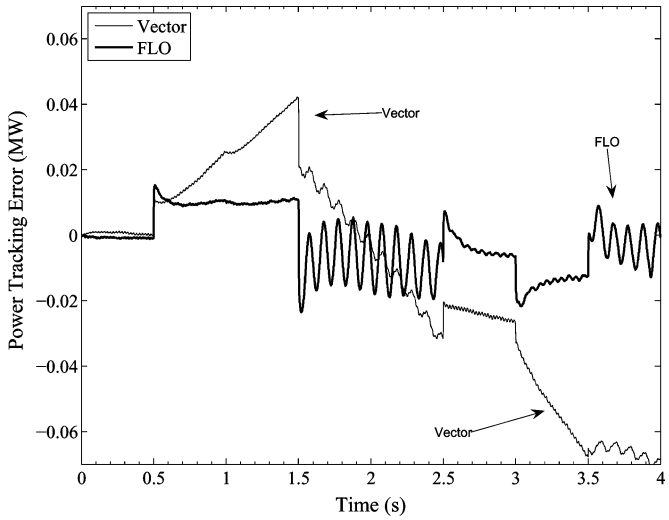

Fig. 4. Active power tracking error with uncertainty: vector control versus FLO.

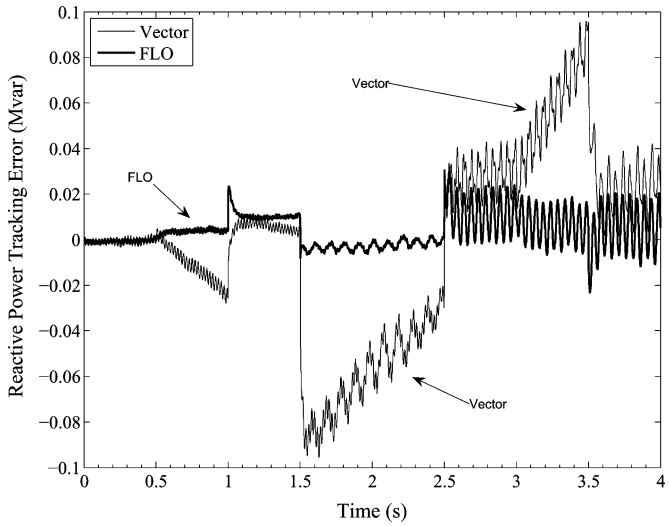

Fig. 5. Reactive power tracking error with uncertainty: vector control versus FLO.

performs relatively well, a larger error associated to speed changes can be noticed compared to the proposed controller.

In Figs. 6 and 7, the FL controller without observer is tested against the proposed controller (FLO) when tracking power references. The active power tracking capability for the FL scheme is better than in the vector control case and approaches that of the FLO performance. However, the uncertainty in rotor-side resistance precludes nonlinearities from being exactly canceled, and the integral action is not enough to prevent these tracking errors, which are bigger than with the proposed FLO controller.

Note that in spite of the important active power changes (1–3 MW), the speed of the DFIM never surpasses 1.1 p.u. and never drops under 0.9 p.u., as shown in Fig. 8. Another important remark is that the VSCs power consumption is always under 25% of the DFIM nominal power, as shown in Fig. 9, even though the rotor resistance is increased by 50%. Finally, the proposed VSC controller has a good performance when tracking the null reactive power reference, as seen in Fig. 9 (bottom subplot).

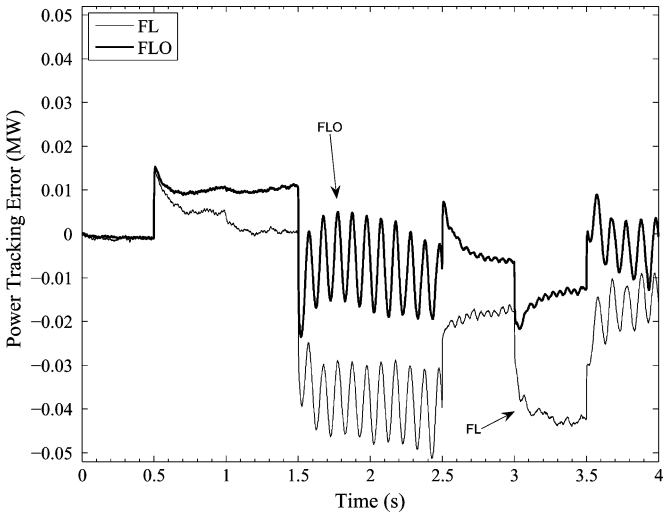

Fig. 6. Active power tracking error with uncertainty: FL versus FLO.

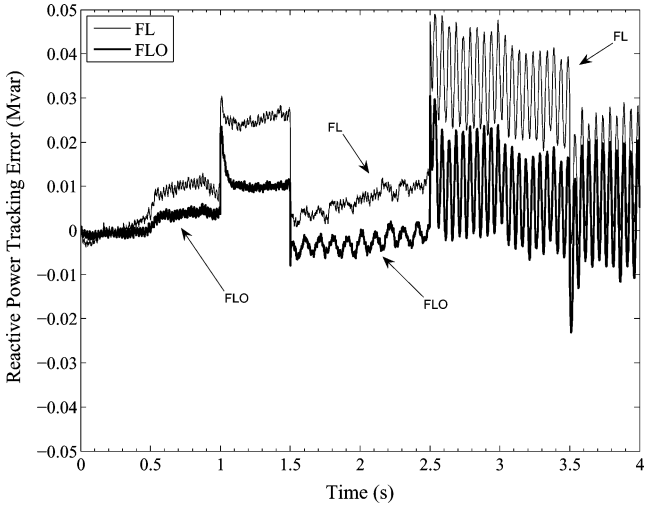

Fig. 7. Reactive power tracking error with uncertainty: FL versus FLO.

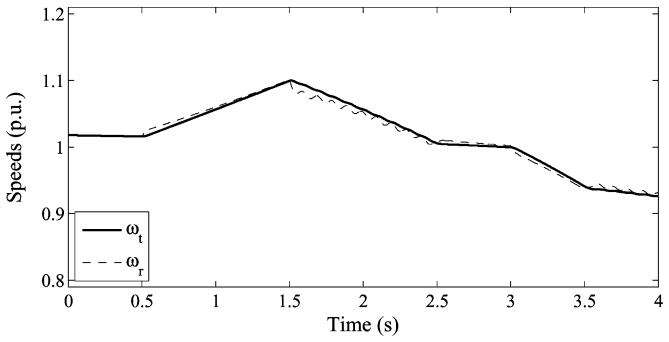

Fig. 8. Turbine and rotor speeds with FLO.

The FL and FLO controllers are tested when their assumed parameter values differ from the actual plant parameters. In order to show the adaptive feature of the proposed FLO controller, a 20% error is considered for the mutual inductance L_m.

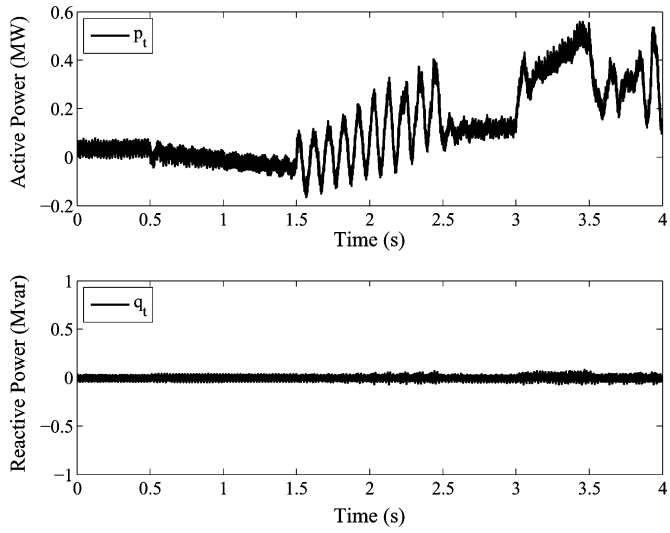

Fig. 9. Stator-side VSC powers with FLO.

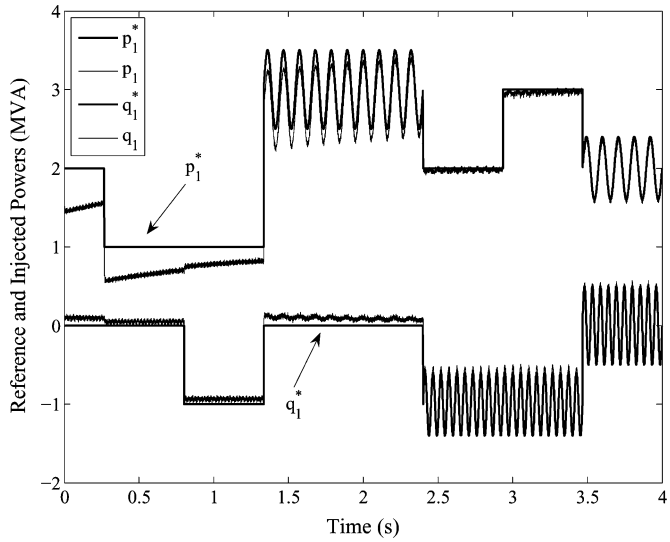

Fig. 10. Active and reactive power tracking with FL and $\Delta L_m = 20\%$.

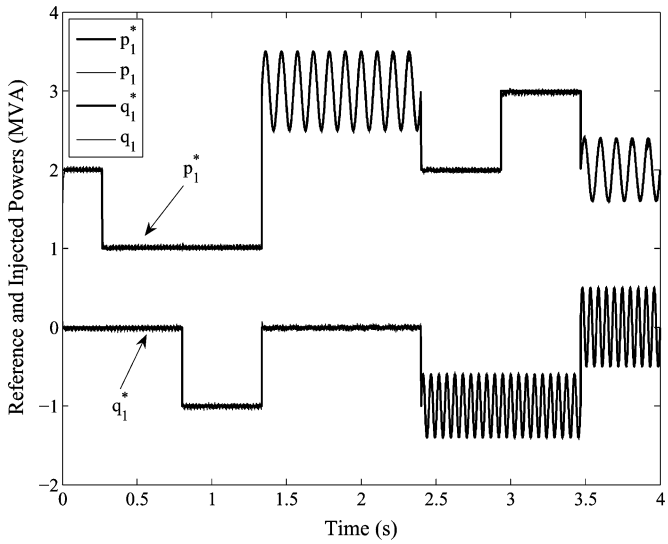

Fig. 11. Active and reactive power tracking with FLO and $\Delta L_m = 20\%$.

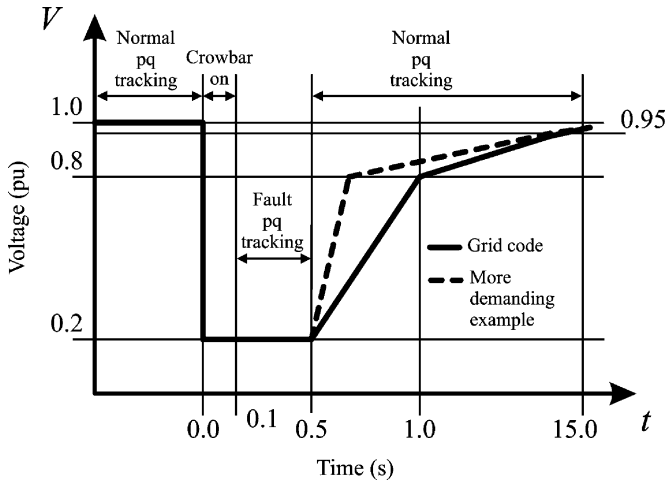

Fig. 12. Voltage at the point of connection.

Analyzing this error is relevant because both stator ($L_s = L_m + L_{ls}$) and rotor ($L_r = L_m + L_{lr}$) inductances depend on this parameter. The tracking performance of the FL controller is shown in Fig. 10. An important initial error arises until the integral term rejects the perturbation. On the other hand, Fig. 11 shows an almost perfect and instantaneous power tracking capability for the FLO controller. There is no steady-state error and the behavior is virtually the same as in the nominal parameter case. A similar performance is obtained when a -20% error in L_m is considered.

B. Fault Mitigation and Parameter Uncertainties

Grid codes for the WEC systems are becoming increasingly demanding regarding this issue. In Fig. 12, a voltage sag at the point of connection is introduced. It is assumed that WEC systems not only have to keep connected during this kind of faults but they should also supply reactive power to the grid in order to support the voltage recovery. The solid line shown in the figure corresponds to a standard voltage sag whereas the dash line is a more demanding case with faster postfault voltage restoration. Controllers may act faster in the second case, in which inrush magnetizing currents are higher. During the fault, the active power reference is set to zero while the reactive power to track is set to 0.2 Mvar. This is a hard requirement, as the low-voltage condition puts the system in an operating state that is far from the normal one.

In all cases, the crowbar protection is activated during the first 100 ms of the voltage sag. This means that the rotor is short circuited through a resistor.

So far as the vector control is concerned, two cases were simulated. In one of the tests, the crowbar protection is not applied when voltage starts recovering after the fault, while in the other case the crowbar is applied for 100 ms once the voltage starts growing. In Figs. 13 and 14, active and reactive power tracking during the fault is shown to be correct but not well damped. When voltage starts recovering, the reactive power is bounded. However, after the fault, when the voltage is still

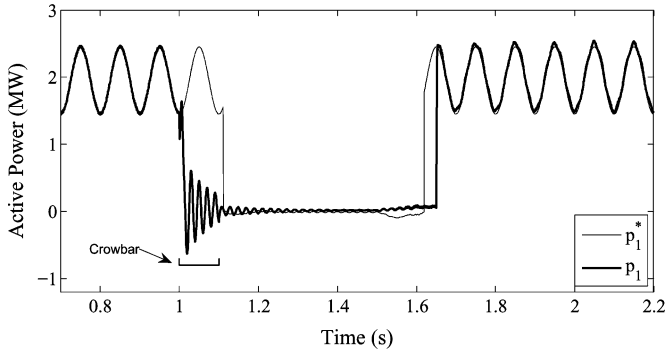

Fig. 13. Fault mitigation and active power reference tracking with vector control.

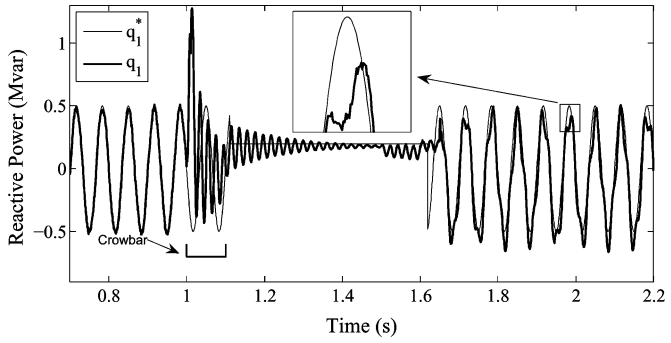

Fig. 14. Fault mitigation and reactive power references tracking with vector control.

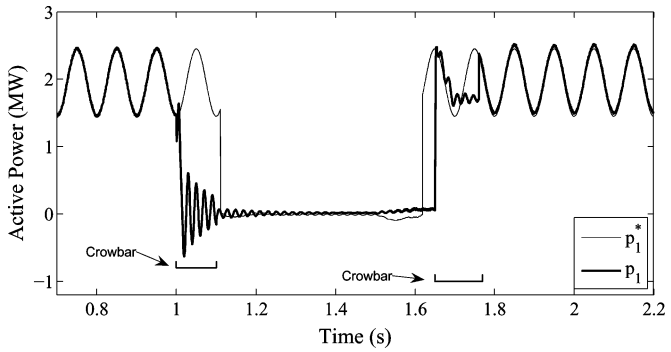

Fig. 15. Fault mitigation and active power reference tracking with vector control and postfault crowbar.

raising, the pq tracking error is important. The same vector control is applied in Figs. 15 and 16 but the crowbar protection is activated twice. After the voltage sag, the pq tracking is much better than in the first case. However, when voltage is recovered, there is an important consumption of reactive power.

In Figs. 17 and 18, the FLO controller is tested against the same voltage sag. The power tracking error is almost zero, as required, its behavior being almost totally damped. Furthermore, when the voltage is partially recovered (0.8 p.u.), there is no extra reactive power consumption and power tracking capability is recovered after about 100 ms. The crowbar action is only required for the first 100 ms of the voltage sag.

The performance of the proposed VSC control to maintain the dc link voltage can be seen in Fig. 19. Even though the voltage sag is applied at ac terminals (dashed line), and the rotor currents are still present, the dc voltage deviation is almost negligible.

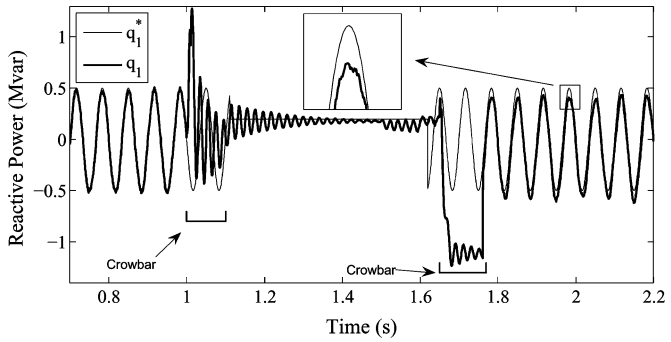

Fig. 16. Fault mitigation and reactive power reference tracking with vector control and postfault crowbar.

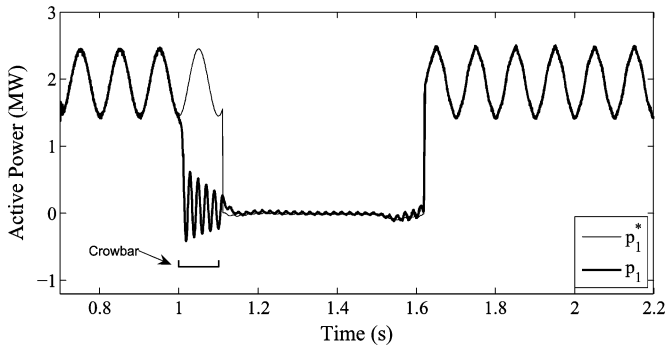

Fig. 17. Fault mitigation and power references tracking with FLO.

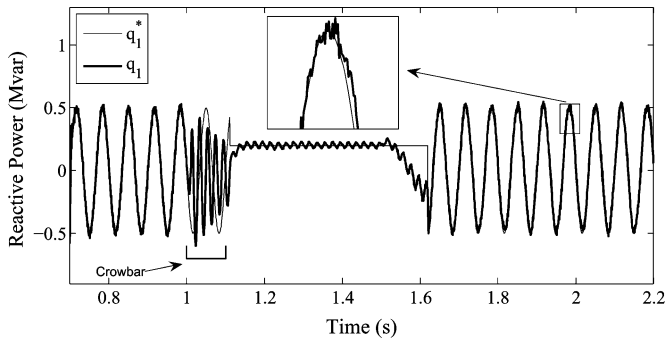

Fig. 18. Fault mitigation and reactive power reference tracking with FLO.

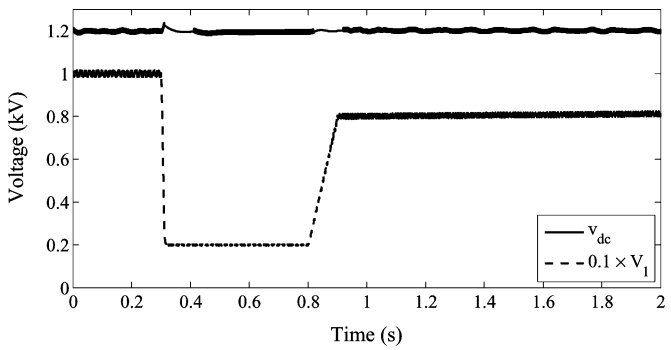

Fig. 19. DC link and bus 1 voltages under normal and fault condition.

V. Conclusion

In this paper, the design of an adaptive controller that improves the performance of the DFIM-based WEC systems under model parameter uncertainties was introduced. This is achieved by the use of a disturbance observer that estimates the model uncertainties (resistances, inductances, converter parameters, etc.), and cancels out their negative effects by including the estimated values in the control law.

Simulations performed in EMTDC/PSCAD show almost exact power reference tracking and good response when close faults are applied. Although the control procedure is more complex than a standard vector-control-based algorithm, both approaches need the same hardware for their implementation. A remarkable feature of the proposed controller is that the DFIM-based WEC system can be used for transiently injecting active and reactive power to the electrical network in a fast way. Such a transient power could be used for power system oscillation damping purposes, as the tracking capability of the proposed controller extends well beyond the typical bandwidth of these oscillations. According to simulations, an added advantage of the proposed scheme is that the crowbar system could be downsized.

Appendix I

Parameters used in the simulations are as follows:

$$\Omega_B = 2\pi 50 Hz, \quad L_m = 3.362 \quad C_{\rm dc} = 7.479$$
$$R_s = 0.0108, \quad L_{ls} = 0.102, \quad L_s = L_m + L_{ls} = 3.46$$
$$R_r = 0.0121, \quad L_{lr} = 0.110, \quad L_r = L_m + L_{lr} = 3.47$$
$$H_t = 2.5\,s, \quad H_r = 0.5\,s, \quad D_{tr} = 5.0 \quad K_{tr} = 0.3.$$

Parameters are in per unit with $S_B = 2$ MVA and $V_B = 0.69$ kV.

References

[1] F. M. Hughes, O. Anaya-Lara, N. Jenkins, and G. Strbac, "Control of DFIG-based wind generation for power network support," *IEEE Trans. Power Syst.*, vol. 20, no. 4, pp. 1958–1966, Nov. 2005.

[2] J. M. Carrasco, L. G. Franquelo, J. T. Bialasiewicz, E. Galvan, R. C. P. Guisado, M. A. M. Prats, J. I. León, and N. Moreno-Alfonso, "Power-electronic systems for the grid integration of renewable energy sources: A survey," *IEEE Trans. Ind. Electron.*, vol. 53, no. 4, pp. 1002–1016, Jun. 2006.

[3] O. C. A. Perdana and J. Persson, "Grid-connected wind turbine with doubly fed induction generator," presented at the Nordic Workshop Power Ind. Electron., Trondheim, Norway, Jun. 2004. vol. 3.

[4] N. R. Ullah and T. Thiringer, "Variable speed wind turbines for power system stability enhancement," *IEEE Trans. Energy Convers.*, vol. 22, no. 1, pp. 52–60, Mar. 2007.

[5] B. Marinescu, "A robust coordinated control of the doubly-fed induction machine for wind turbines: A state-space based approach," in *Proc. 2004 Amer. Control Conf.*, Jun. 2004, vol. 1, pp. 174–179.

[6] L. S. Barros, W. S. Mota, and D. F. P. Moura, "Matrix method to linearization and state space representation of power systems containing doubly fed induction machines operating as wind generators," in *Proc. IEEE/PES Trans. Distrib. Conf. Expo.: Latin America*, Aug. 2006, pp. 1–6.

[7] W. Leonhard, *Control of Electrical Drives*, 3rd ed. New York: Springer-Verlag, 2001.

[8] R. G. de Almeida, J. A. P. Lopes, and J. A. L. Barreiros, "Improving power system dynamic behavior through doubly fed induction machines controlled by static converter using fuzzy control," *IEEE Trans. Power Syst.*, vol. 19, no. 4, pp. 1942–1950, Nov. 2004.

[9] C. Batlle, A. Doria-Cerezo, and R. Ortega, "Power flow control of a doubly-fed induction machine coupled to a flywheel," in *Proc. 2004 IEEE Int. Conf. Control Appl.*, Sep., vol. 2, pp. 1645–1650.

[10] S. Peresada, A. Tilli, and A. Tonielli, "Robust active–reactive power control of a doubly-fed induction generator," in *Proc. IEEE Ind. Electron. Soc. IECON 1998*, Aug., vol. 3, pp. 1621–1625.

[11] D. Zhi and L. Xu, "Direct power control of DFIG with constant switching frequency and improved transient performance," *IEEE Trans. Energy Convers.*, vol. 22, no. 1, pp. 110–118, Mar. 2007.

[12] A. Isidori, *Nonlinear Control Systems. An Introduction*, 3rd ed. London, Great Britain: Springer-Verlag, 1995.

[13] J. Solsona, M. I. Valla, and C. Muravchik, "Nonlinear control of a permanent magnet synchronous motor with disturbance torque estimation," *IEEE Trans. Energy Convers.*, vol. 15, no. 2, pp. 163–168, Jun. 2000.

[14] N. P. Quang, A. Dittrich, and P. N. Lan, "Doubly-fed induction machine as generator in wind power plant: Nonlinear control algorithms with direct decoupling," in *Proc. Eur. Conf. Power Electron. Appl.*, Sep. 2005, pp. 1–10.

[15] D. D. Li and C. Chen, "Decoupled control of speed and reactive power of doubly-fed induction generator," in *Proc. PowerCon 2004. Inter. Conf. Power Syst. Technol.*, Nov. 2004, vol. 1, pp. 356–360.

[16] J. Soltani, A. F. Payam, and M. A. Abbasian, "A speed sensorless sliding-mode controller for doubly-fed induction machine drives with adaptive backstepping observer," in *Proc. ICIT 2006. IEEE Int. Conf. Ind. Technol.*, Dec. 2006, pp. 2725–2730.

[17] J. Morren and S. W. H. de Haan, "Short-circuit current of wind turbines with doubly fed induction generator," *IEEE Trans. Energy Convers.*, vol. 22, no. 1, pp. 174–180, Mar. 2007.

[18] V. Akhmatov, "Analysys of dynamic behaviour of electric power system with large amount of wind power," Ph.D. dissertation, Technical Univ. of Denmark, Lyngby, Denmark, Apr. 2003.

[19] A. Tapia, G. Tapia, J. X. Ostolaza, and J. R. Sáenz, "Modeling and control of a wind turbine driven doubly fed induction generator," *IEEE Trans. Energy Convers.*, vol. 18, no. 2, pp. 194–204, Jun. 2003.

[20] S. K. Salman and A. L. J. Teo, "Windmill modeling consideration and factors influencing the stability of a grid-connected wind power-based embedded generator," *IEEE Trans. Power Syst.*, vol. 18, no. 2, pp. 793–802, May 2003.

[21] J.-J. E. Slotine and W. Li, *Applied Nonlinear Control*. Englewood Cliffs, NJ: Prentice-Hall, 1991.

[22] H. Akagi, Y. Kanazawa, and A. Nabae, "Generalized theory of the instantaneous reactive power in three-phase circuits," in *Proc. Int. Power Electron. Conf. (IPEC) 1983*, Tokyo, Japan, pp. 1375–1386.

[23] N. Mendalek, K. Al-Haddad, F. Fnaiech, and L. A. Dessaint, "Nonlinear control technique to enhance dynamic performance of a shunt active power filter," in *Proc. Inst. Electr. Eng. Electr. Power Appl.*, Jul. 2003, vol. 150, pp. 373–379.

[24] P. Kundur, *Power System Stability and Control*. New York: McGraw-Hill, 1994.

Juan Manuel Mauricio (S'01) was born in Argentina in 1977. He received the Degree in electrical engineering from the National University of Comahue, Neuquén, Argentina, in 2003. He is currently working toward the Ph.D. degree in electrical engineering at the University of Seville, Seville, Spain.

His current research interests include power systems modeling and control and FACTS.

Andrés E. León (S'05) was born in Argentina in 1979. He received the Degree in electrical engineering from the National University of Comahue, Neuquén, Argentina, in 2005. He is currently working toward the Ph.D. degree in control systems at the Instituto de Investigaciones en Ingeniería Eléctrica (IIIE), Universidad Nacional del Sur, Bahía Blanca, Argentina.

His current research interests include power systems modeling and control and Flexible Alternating Current Transmission Systems (FACTS).

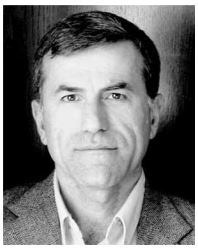

Antonio Gómez-Expósito (M'97–SM'95–F'05) was born in Spain in 1957. He received the Electrical and Doctor of Engineering degrees from the University of Seville, Seville, Spain, in 1982 and 1985, respectively.

Since 1982, he has been with the Department of Electrical Engineering, University of Seville, where he is currently a Professor and the Chairman. His current research interests include power system optimization, state estimation, and digital signal processing.

Jorge A. Solsona (SM'04) received the Electronics Engineer and Doctor degrees from the Universidad Nacional de La Plata, La Plata, Argentina, in 1986 and 1995, respectively.

He is currently with the Instituto de Investigaciones en Ingeniería Eléctrica Alfredo Desages, Departamento de Ingeniería Eléctrica y de Computadoras, Universidad Nacional del Sur, Bahía Blanca, Argentina and Consejo Nacional de Investigaciones Científicas y Técnicas (CONICET), where he is engaged in teaching and research on control theory and its applications to electromechanical systems.